Fuel 89 (2010) 336–345

Contents lists available at ScienceDirect

Fuel

journal homepage: www.elsevier.com/locate/fuel

Kerogen pyrolysis in the presence and absence of water and minerals: Steranes and triterpenoids

Changchun Pan [a,*], Ansong Geng [a], Ningning Zhong [b], Jingzhong Liu [a]

[a] State Key Laboratory of Organic Geochemistry, Guangzhou Institute of Geochemistry, Chinese Academy of Sciences, Wushan, Guangzhou 510640, PR China
[b] Faculty of Natural Resource and Information Technology, The University of Petroleum, Beijing 102249, PR China

ARTICLE INFO

Article history:
Received 7 January 2009
Received in revised form 31 May 2009
Accepted 25 June 2009
Available online 12 July 2009

Keywords:
Confined pyrolysis on kerogen
Mineral catalysis
Steranes and triterpenoids

ABSTRACT

This paper documents the distribution and maturation behavior of hopanoids and steranes released from kerogen (Estonian Kukersite) during pyrolysis experiments, performed in confined system (gold capsule) in presence and absence of water and various minerals, kaolinite, montmorillonite, calcite and dolomite respectively, at a fixed pressure of 50 MPa and temperature ranging from 240–320 °C. The abundances of hopenes and 17β(H)21β(H)-hopanes relative to stable 17α(H)21β(H)-hopanes, as well as calculated maturity parameters obtained from steranes and homohopanes are significantly different for the studied kerogen mixed with different minerals, and the presence or absence of water. The results of our experiments show that the maturation rates of hopanoids and steranes increase with mineral acidity but decrease with the addition of water. Furthermore, the stabilities of hopenes relative to 17β(H)21β(H)-hopanes also vary significantly at a same temperature among the six runs. Hopenes are more sensitive to the addition of excessive amount of water and pH value of minerals than are 17β(H)21β(H)-hopanes.

1. Introduction

Biomarkers are complex molecular fossils derived from biochemicals, particularly lipids, in once-living organisms [1]. The origins and maturation of these molecules, especially steroids and terpanoids, have been extensively studied and the results have been widely applied in petroleum geochemistry [1–9]. Previous studies have revealed that steroids and hopanoids which are bound to kerogen via heteroatomic cross-links have low maturities compared with their free counterparts [10–15]. The overall maturity of biomarkers for a source rock depends on the release behavior of kerogen-bound compounds and the maturation of the free ones. Previous experimental studies have demonstrated that the generation and maturation of biomarker compounds can be significantly affected by water and minerals [11,16–21]. For instance, Koopmans et al. noticed that anhydrous pyrolysis of a claystone containing II-S kerogen did not generate biomarkers, strikingly different from hydrous pyrolysis. In contrast, only slight difference was observed in biomarker generation between hydrous and anhydrous pyrolysis on a limestone containing II-S kerogen. These authors believed that both water and mineral matrix play an important role in biomarker generation [20]. Sieskind et al. found that the anhydrous transformation of cholestanol into steranes and sterenes was catalyzed by superacid sites present in kaolinite and montmorillonite [16]. Alexander et al. proposed a clay-catalyzed reaction mechanism for alkyl hydrogen exchange based on the result of anhydrous heating experiments (160 °C) on tritium-labelled cumenes plus homoionic montmorillonite [17]. Tannenbaum et al. and Lu et al. observed that the isomerization rates of terpanes and steranes increase in the presence of montmorillonite during anhydrous kerogen pyrolysis [18,19]. Peters et al. performed a hydrous pyrolysis study on two immature Monterey source rocks, i.e. phosphatic and siliceous, and found that these two source rocks can show different sterane or hopane isomerization ratios when heated under the same time/temperature condition, and therefore, believed that rock mineralogy could influence the biomarker maturation [11]. Lewan demonstrated that the maturation rates of biomarkers (terpanes, steranes, monoaromatic and triaromatic steranes) were retarded under hydrous conditions in comparison with anhydrous conditions [21]. Hopane and sterane distributions are widely used as the source and maturity parameters, and for oil-source correlations [1,4–6]. An extensive understanding of how, and to what extent, the mineral matrix and water influence the generation and maturation of these biomarkers is vital for the proper application of the biomarker parameters for thermal maturity. In this paper, we document the release and maturation behavior of terpanoids and steranes during our pryolysis experiments on kerogen in the absence and presence of water and minerals.

* Corresponding author. Tel.: +86 20 85290183; fax: +86 20 85290706.
E-mail address: cpan@gig.ac.cn (C. Pan).

0016-2361/$ - see front matter © 2009 Elsevier Ltd. All rights reserved.
doi:10.1016/j.fuel.2009.06.032

2. Experimental

2.1. Samples

The kerogen used for this study was separated from the Estonian Ordovician immature oil shale (Kukersite). After Soxhlet extraction of the powdered sample (about 200 mesh) of the oil shale with an azeotropic mixture of dichloromethane:methanol (93:7 vol/vol) for 72 h, the sample was treated with HCl (6 N) and HF:HCl (1:1) to remove carbonate and silicate minerals. The detailed procedure for the kerogen preparation was given elsewhere [22,23]. This Kukersite oil shale sample is rich in organic matter with the total organic carbon content (TOC) 47.4%, and contains 16.7% carbonate minerals and 13.0% silicate and other minerals. TOC of the kerogen obtained was 67.40%.

Four minerals were used in this study, i.e. kaolinite, montmorillonite (Ca/Na mixed), calcite and dolomite. The pH values for these four minerals measured in mud (mineral:de-ionized water 1:5 wt.) at 25 °C were kaolinite 4.99, montmorillonite 9.88, calcite 9.11 and dolomite 8.84. About 1.5 g dry Kukersite kerogen was mixed with about 24 g of each of the above four minerals given four mixtures with TOC of about 4 wt.%. The detailed procedure for the preparation of mineral–kerogen mixtures was given in our previous papers [22,23].

2.2. Pyrolysis experiments

All pyrolysis experiments were conducted in flexible gold capsules (4 mm outside diameter, 0.25 mm wall thickness and 4 cm or 6 cm length) contained within steel pressure vessels. The shorter capsules (4 cm length) were used for loading kerogen alone (about 60 mg) or kerogen (about 60 mg) plus the same amount of de-ionized water, while the longer ones (6 cm length) were used for loading kerogen plus mineral and de-ionized water (470.90–673.12 mg solid and 200 mg of de-ionized water).

The vessels were previously filled with water. Two capsules were placed into each vessel. The internal pressure of the vessels, which were connected to each other with pipelines, was adjusted to 50 MPa by pumping water into the vessels before heating. It maintained automatically by pumping water into or out of the vessels during pyrolysis experiments. Five series of pyrolysis experiments were conducted at temperatures of 240, 280, 320, 360, and 400 °C, respectively. For each of the runs, 12 capsules (240–360 °C) or 15 capsules (400 °C) loaded with six types of samples and duplicates were placed into six or eight pressure vessels. The vessels were heated to the desired temperature within 2 h, and then held isothermally for 72 h.

2.3. GC–MS analysis

After pyrolysis experiments, 24 capsules were used for gaseous hydrocarbon analysis. The remaining 36 capsules were used for liquid hydrocarbon analysis. The analytical results of the gaseous and liquid products have been reported elsewhere [22,23]. After both analyses, samples within the 60 capsules were Soxhlet extracted with azeotrope of dichloromethane:methanol (93:7 vol/vol) for 72 h.

The Soxhlet extracts, obtained from the initial oil shale prior to heating and samples within the capsules after heating were deasphaltened by the addition of about 40-fold n-hexane. The maltenes were fractionated on a silica-alumina column using hexane and benzene as eluants to yield the aliphatic and aromatic fractions respectively. Solvents were recovered using a rotary vacuum evaporator and fractions were transferred into vials and dried thoroughly in a stream of nitrogen.

The GC–MS analyses of the 36 saturate fractions of Soxhlet extracts from the initial oil shale and samples within the capsules heated at the temperatures of 240–320 °C were at first carried out using a Micromass Plateform II interfaced to an HP5890 GC fitted with a 30 m × 0.25 mm.i.d. HP-5 column with a 0.25 μm film thickness. Helium was used as the carrier gas. The GC oven temperature was initially held at 60 °C for 5 min, ramped from 60 to 120 °C at 8 °C/min, from 120 to 290 °C at 2 °C/min, and then held isothermally at 290 °C for 30 min. A full scan (*m/z* 50 to *m/z* 600) detection approach was used. The runs were repeated in multiple-ion detection (MID) mode under the same analytical conditions but using a 30 m × 0.25 mm.i.d. DB-5 ms column with a 0.25 μm film thickness. This enhances the peak intensities of *m/z* 191 and *m/z* 217 mass chromatograms by about ten folds.

3. Results

3.1. Terpenoids and steranes from the solvent extract of the initial Kukersite oil shale

The *m/z* 191 and *m/z* 217 mass chromatograms of the solvent extract from the initial oil shale and samples pyrolysed at 240, 280, and 320 °C, obtained in the MID mode, are shown in Figs. 1–3. The peak assignments on these figures are given in Table 1. Thirteen molecular parameters obtained from these GC–MS analyses are listed in Table 2. Among them, four ratios demonstrating the concentrations of hopenes, and 17β(H)21β(H)-hopanes relative to 17α(H)21β(H)-hopanes, are plotted in Fig. 4. Other four ratios of $C_{31}22S/(22R+22S)$ homohopanes, $C_{29}20S/(20R+20S)$ steranes, $C_{29}\alpha\beta\beta/(\alpha\alpha\alpha+\alpha\beta\beta)$ steranes, and 17β(H),21α(H)-hopane/17α(H),21β(H)-hopane are plotted in Fig. 5.

As shown in Fig. 1, for the original bitumen, the abundance of 22,29,30-trisnorneohop-13(18)-ene is considerably high, nearly one half of 17αH,22,29,30-trisnorhopane while the abundance of 22,29,30-trisnorhop-17(21)-ene is substantially low.

The amount of 30-norneohop-13(18)-ene is also very high, and the (30-norneohop-13(18)-ene + 30-norhop-17(21)-ene)/17α(H),21β(H)-30-norhopane ratio is 2.032. Although 30-norhop-17(21)-ene co-elutes with 17α(H),21β(H)-30-norhopane, the amount of 30-norhop-17(21)-ene relative to 30-norneohop-13(18)-ene and 17α(H),21β(H)-30-norhopane is extremely too low for detection as verified using *m/z* 396 and *m/z* 398.

Both hop-17(21)-ene and neohop-13(18)-ene, especially the latter, are significantly high, and the ratios of hop-17(21)-ene/17α(H),21β(H)-hopane and neohop-13(18)-ene/17α(H),21β(H)-hopane are 0.14 and 0.60 respectively (Table 2 and Fig. 1).

The ratios of 17β(H),22,29,30-trisnorhopane/17α(H),22,29,30-trisnorhopane and 17β(H)21β(H)-hopane/17α(H),21β(H)-hopane are considerably high, 0.86 and 0.21 respectively. However, the amount of 17β(H)21β(H)-30-norhopane is almost below the detection limit in *m/z* 191 mass chromatogram (Fig. 1). The presence of triterpenes and 17β(H)21β(H)-hopane in significant amounts in the original bitumen indicates that the initial oil shale is apparently immature [1–6].

The ratio of $C_{31}22S/(22R+22S)$ homohopanes is 0.36, which is lower than the equilibrium value of 0.60 [5,22]. Both the ratios of $C_{29}20S/(20R+20S)$ and $C_{29}\alpha\beta\beta/(\alpha\alpha\alpha+\alpha\beta\beta)$ steranes are also very low, 0.12 and 0.25 respectively (Table 2 and Fig. 1). These ratios also demonstrate the low maturity of the initial oil shale [6,22].

3.2. Terpenoids and steranes of pyrolysates at 240 °C

The distributions of terpenoids and steranes are significantly different among the six experiments (Fig. 1). The six experiments can be classified into two groups based on the terpenoid and ster-

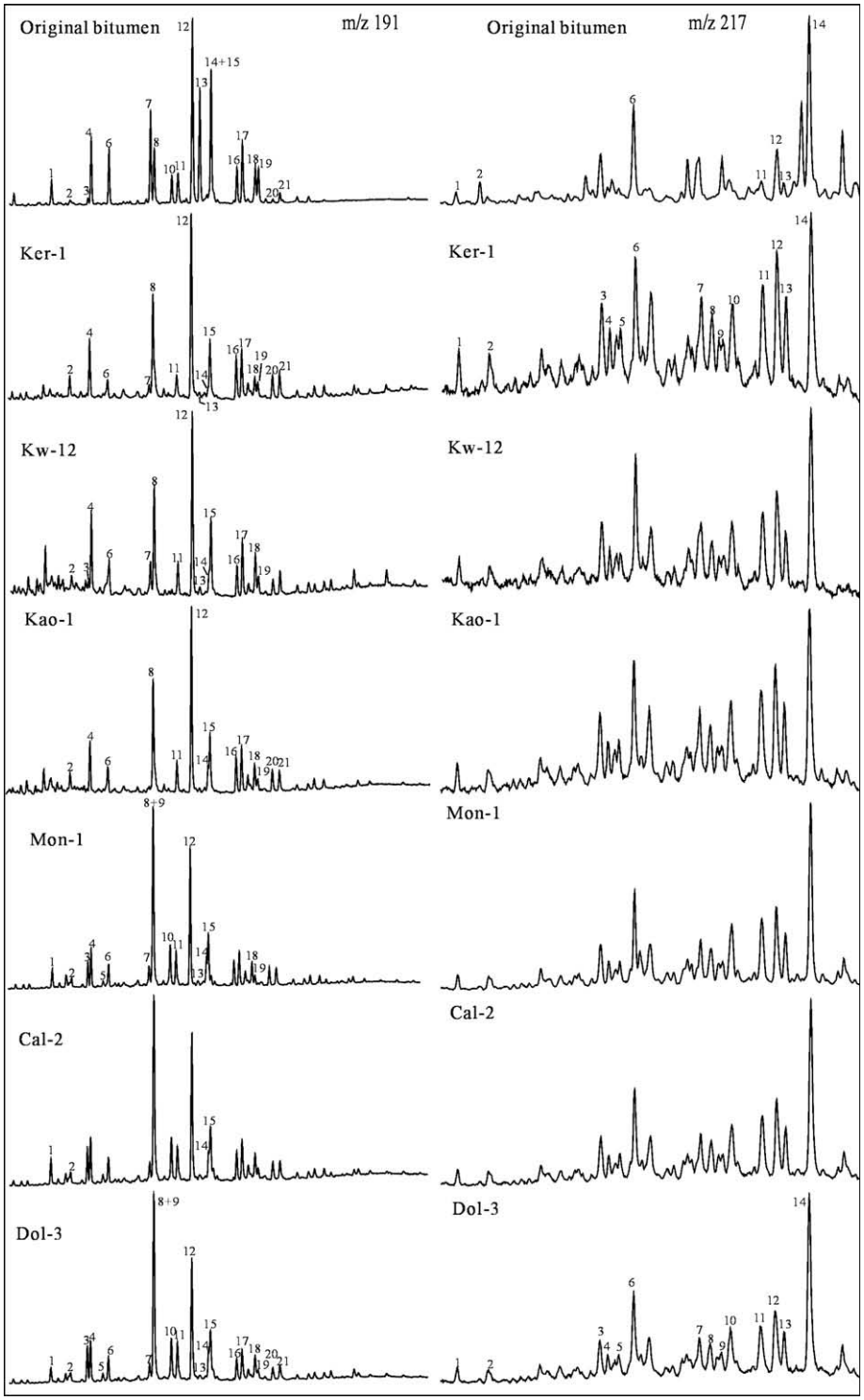

Fig. 1. *m/z* 191 and *m/z* 217 mass chromatograms of solvent extract from the initial oil shale prior to heating and pyrolysates produced at temperature 240 °C. Original bitumen: extract from the initial oil shale; Ker-1, Kw-12, Kao-1, Mon-1, Cal-2 and Dol-3 see Table 2; Peak assignments are given in Table 1.

ane distributions. The group 1 includes the three experiments for kerogen alone, using de-ionized water only and using kaolinite. Group 2 includes the other three experiments using montmorillonite, calcite and dolomite, respectively.

In group 1, the concentrations of 22,29,30-trisnorneohop-13(18)-ene, 22,29,30-trisnorhop-17(21)-ene and hop-17(21)-ene are very low, some even below detection limit as in sample pyrolysed in presence of kaolinite. In contrast, to group 2, the concentrations of these terpenes are very high with the ratios of trisnorhopenes/trisnorhopanes and hop-17(21)-ene/17α(H),21β(H)-hopane ranging from 0.70 to 0.83 and from 0.32 to 0.45, respectively (Table 2, Fig. 4a and b).

30-Norhop-17(21)-ene is below detection limit in group 1, while in group 2, it is highly abundant. The ratio (30-norneohop-13(18)-ene + 30-norhop-17(21)-ene)/17α(H),21β(H)-30-norhopane starts from 1.22 to 1.59, as determined from *m/z* 396 and *m/z* 398

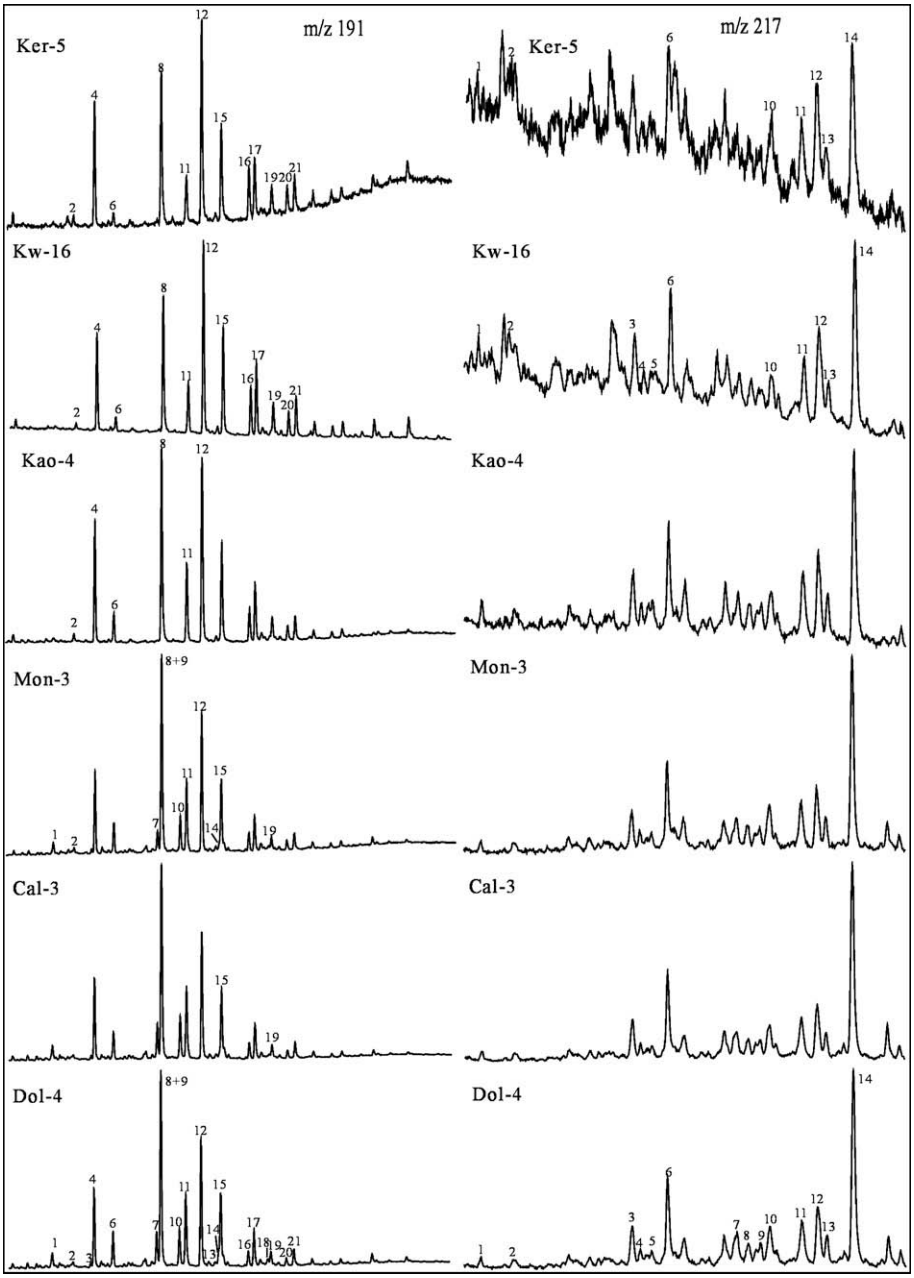

Fig. 2. *m/z* 191 and *m/z* 217 mass chromatograms of pyrolysates produced at temperature 280 °C. Ker-5, Kw-16, Kao-4, Mon-3, Cal-3 and Dol-4 see Table 2; Peak assignments are given in Table 1.

mass chromatograms (Table 2). However, the concentration of 30-norneohop-13(18)-ene in the presence of de-ionized water (group 1) appears exceptional, higher than in group 2 (Fig. 1).

In group 2, an unknown trisnorhopene is detected in trace amount while it is absent in group 1 and in the original bitumen prior to heating (Fig. 1).

In both groups, the abundances of 17β(H), 22,29,30-trisnorhopane, 17β(H)21β(H)-30-norhopane and 17β(H)21β(H)-hopane relative to their stable counterparts 17α(H), 22,29,30-trisnorhopane, 17α(H)21β(H)-30-norhopane and 17α(H)21β(H)-hopane are significantly high. However, they appear to be relatively lower in the experiment for kerogen alone than in the other experiments (Table 2, Figs. 1 and 4c and d).

The ratio of $C_{31}22S/(22R + 22S)$ homohopanes ranges 0.36–0.45, and the ratios of $C_{29}20S/(20R + 20S)$ and $C_{29}\alpha\beta\beta/(\alpha\alpha\alpha + \alpha\beta\beta)$ steranes range 0.25–0.40 and 0.31–0.42, respectively, among the six experiments. These ratios are generally higher in the group 1 than group 2 except that the ratios of $C_{31}22S/(22R + 22S)$ homohopanes is lower in the presence of de-ionized water only (group 1) than in the other experiments (Table 2 and Fig. 5a–c).

3.3. Terpenoids and steranes of pyrolysates at 280 °C

All C_{27}, C_{29} and C_{30} triterpenes are undetectable in the group 1, however, they are present in the group 2 (Table 2 and Fig. 2). Although 22,29,30-trisnorhop-17(21)-ene is only present in trace amount, 22,29,30-trisnorneohop-13(18)-ene, 30-norneohop-13(18)-ene, 30-norhop-17(21)-ene and hop-17(21)-ene remain in significant amount in the group 2 (Table 2, Figs. 2 and 4a and b).

In both groups, 17β(H)21β(H)-30-norhopane and 17β(H)21β(H)-hopane are undetectable, or are only in trace amount (Table 2 and Figs. 2 and 4c and d). However, the concentration of 17β(H),

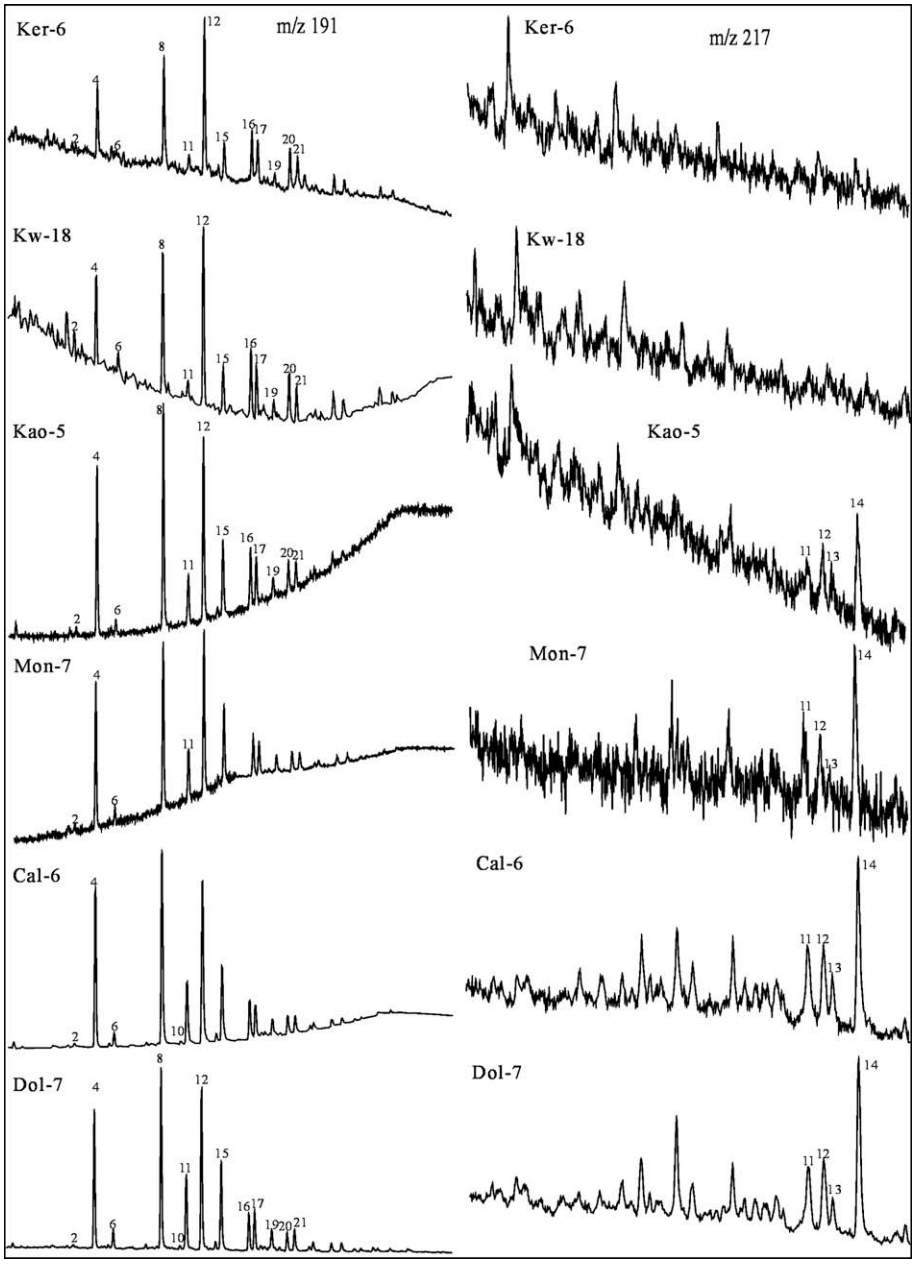

Fig. 3. *m/z* 191 and *m/z* 217 mass chromatograms of pyrolysates produced at temperature 320 °C. Ker-6, Kw-18, Kao-5, Mon-7, Cal-6 and Dol-7 see Table 2; Peak assignments are given in Table 1.

22,29,30-trisnorhopane relative to 17α(H),22,29,30-trisnorhopane is significantly high in both groups, and relatively lower in group 1 than in group 2 (Figs. 2 and 4c).

The ratios of $C_{31}22S/(22R+22S)$ homohopanes, $C_{29}20S/(20R+20S)$ and $C_{29}\alpha\beta\beta/(\alpha\alpha\alpha+\alpha\beta\beta)$ steranes range from 0.29–0.46, 0.21–0.36 and 0.26–0.43 respectively in the six experiments (Table 2). All the three ratios are higher in the group 1 than in the group 2 (Table 2 and Fig. 5a–c).

3.4. Terpenoids and steranes of pyrolysates at 320°C

All C_{27}, C_{29} and C_{30} triterpenes are undetectable in group 1. Only trace amounts of 22,29,30-trisnorneohop-13(18)-ene, 30-norneohop-13(18)-ene and hop-17(21)-ene are present in group 2 (Table 2, Figs. 3 and 4).

In both groups, 17β(H)21β(H)-30-norhopane and 17β(H)21β(H)-hopane are in trace amount. However, 17β(H),22,29,30-trisnorhopane is present in considerable amounts in both groups (Figs. 3 and 4c and d).

The abundances of 17α(H), 22,29,30-trisnorhopane and 17α(H)21β(H)-30-norhopane relative to 17α(H)21β(H)-hopane, and the abundances of 17β(H)21α(H)-30-norhopane and 17β(H)21α(H)-hopane relative to 17α(H)21β(H)-30-norhopane and 17α(H)21β(H)-hopane are relatively lower in the two experiments for kerogen alone and in the presence of de-ionized water only than in the other four experiments (Figs. 3 and 5d).

The ratio of $C_{31}22S/(22R+22S)$ homohopanes ranges from 0.48 to 0.62 among the six experiments and is higher in group 1 than in group 2 (Table 2, Fig. 5a). Steranes are only present in the four experiments in the presence of minerals (Fig. 3). The ratios of $C_{29}20S/(20R+20S)$ and $C_{29}\alpha\beta\beta/(\alpha\alpha\alpha+\alpha\beta\beta)$ steranes range 0.29–0.41 and 0.30–0.44 respectively in the four experiments and both are significantly higher in the experiments using kaolinite (group 1) than in group 2 (Table 2 and Fig. 5b and c).

Table 1
Terpane and sterane identifications in Figs. 1–3.

Peak	Identification	Carbon number
	m/z 191	
1	22,29,30-trisnorneohop-13(18)-ene	27
2	18α(H),22,29,30-trisnorhopane–Ts	27
3	22,29,30-trisnorhop-17(21)-ene	27
4	17α(H),22,29,30-trisnorhopane–Tm	27
5	unknown trisnorhopene	27
6	17β(H),22,29,30-trisnorhopane	27
7	30-norneohop-13(18)-ene	29
8	17α(H),21β(H)-30-norhopane	29
9	30-norhop-17(21)-ene	29
10	hop-17(21)-ene	30
11	17β(H)21α(H)-30-norhopane	29
12	17α(H),21β(H)-hopane	30
13	neohop-13(18)-ene	30
14	17β(H)21β(H)-30-norhopane	29
15	17β(H),21α(H)-hopane	30
16	17α(H),21β(H)-homohopane (22*S*)	31
17	17α(H),21β(H)-homohopane (22*R*)	31
18	17β(H)21β(H)-hopane	30
19	17β(H),21α(H)-homohopane	31
20	17α(H),21β(H)-bishomohopane (22*S*)	32
21	17α(H),21β(H)-bishomohopane (22*R*)	32
	m/z 217	
1	13β(H), 17α(H)-diacholestane (20*S*)	27
2	13β(H), 17α(H)-diacholestane (20*R*)	27
3	5α(H), 14α(H), 17α(H)-cholestane (20*S*)	27
4	5α(H), 14β(H), 17β(H)-cholestane (20*R*)	27
5	5α(H), 14β(H), 17β(H)-cholestane (20*S*)	27
6	5α(H), 14α(H), 17α(H)-cholestane (20*R*)	27
7	24-methyl-5α(H), 14α(H), 17α(H)-cholestane (20*S*)	28
8	24-methyl-5α(H), 14β(H), 17β(H)-cholestane (20*R*)	28
9	24-methyl-5α(H), 14β(H), 17β(H)-cholestane (20*S*)	28
10	24-methyl-5α(H), 14α(H), 17α(H)-cholestane (20*R*)	28
11	24-ethyl-5α(H), 14α(H), 17α(H)-cholestane (20*S*)	29
12	24-ethyl-5α(H), 14β(H), 17β(H)-cholestane (20*R*)	29
13	24-ethyl-5α(H), 14β(H), 17β(H)-cholestane (20*S*)	29
14	24-ethyl-5α(H), 14α(H), 17α(H)-cholestane (20*R*)	29

4. Discussion

4.1. Stabilities of hopenes and 17β(H)21β(H)-hopanes

Hopenes and 17β(H)21β(H)-hopanes are found in recent sediments or/and in immature sediments. During diagenesis, a process through which the loose sediment normally becomes consolidated, these compounds are unstable and can be converted to stable hopanes or decompose to yield other products [1,5,6,24–29]. It has been proposed that hop-17(21)-enes can be converted to neohop-13(18)-enes by isomerization [24–26]. Therefore, the latter are more stable than the former during diagenesis. Shi et al. indicated that in immature sediments, with increasing burial or thermal stress, 17β(H)21β(H)-hopanes tend to be more stable than hopenes [29].

The solvent extract from the initial oil shale prior to heating contains relatively more neohop-13(18)-enes and less hop-17(21)-enes than do the pyrolysates produced in the group 2 at 240 °C. One possible explanation for this phenomenon is that most hop-17(21)-enes in the original bitumen, especially 22,29,30-trisnorhop-17(21)-ene and 30-norhop-17(21)-ene, have been converted to neohop-13(18)-enes [24–26], or have decomposed into other products during diagenesis.

30-Norneohop-13(18)-ene is observed to transform in a manner that is different from other hopenes. The relative abundance of 30-norneohop-13(18)-ene is higher in the experiment using de-ionized water only than in the other experiment at 240 °C and it increases slightly from 240 °C to 280 °C in group 2 (Figs. 1 and 2). This result also indicates that some 30-norneohop-13(18)-ene was converted from 30-norhop-17(21)-ene during pyrolysis experiments as suggested in the previous studies [24–26].

The high abundance of hop-17(21)-enes compared to neohop-13(18)-enes indicates that the kerogen primarily released hop-17(21)-enes during pyrolysis in group 2 at 240 °C (Fig. 1). The substantially higher abundance of hopenes in group 2 than in group 1 demonstrates that hopenes are peculiarly stable in group 2 during pyrolysis at 240 °C to 280 °C.

In contrast to hopenes, 17β(H)21β(H)-hopanes are present in a relatively similar amount at 240 °C and have almost disappeared at 280 °C in both groups. This result suggests that the stabilities of 17β(H)21β(H)-hopanes relative to hopenes is significantly different between the groups 1 and 2. In the two experiments for kerogen alone and in the presence of kaolinite (group 1), 17β(H)21β(H)-hopanes are obviously more stable than are all hopenes. In contrast, it is exactly opposite in the group 2. As to the experiment in the presence of de-ionized water (group 1), 17β(H)21β(H)-hopanes are more stable than are hop-17(18)-enes while the same stable as 30-norneohop-13(18)-ene. This result indicates that hopenes are more sensitive to the addition of excessive amount of water and pH value of minerals than are 17β(H)21β(H)-hopanes during our pyrolysis experiments.

4.2. Variation trend of the ratios of $C_{31}22S/(22R+22S)$ homohopanes and $C_{29}20S/(20R+20S)$ and $C_{29}\alpha\beta\beta/(\alpha\alpha\alpha+\alpha\beta\beta)$ steranes

According to the results of our experiments (Table 2 and Fig. 5a–c), it can be generalized that, (1) these three ratios are higher in group 1 than in group 2 except that the ratio of $C_{31}22S/(22R + 22S)$ homohopanes is relatively low in the experiments for kerogen alone and using de-ionized water only at 240 °C; (2) these three ratios at first decrease from 240 °C to 280 °C, and then, increase from 280 °C to 320 °C for all experiments except that the ratios of $C_{31}22S/(22R + 22S)$ homohopanes and $C_{29}\alpha\beta\beta/(\alpha\alpha\alpha + \alpha\beta\beta)$ steranes increase in the experiments for kerogen alone and using de-ionized water only from 240 °C to 280 °C.

These three ratios are widely used as thermal maturity indicators for both source rocks and oils [1,4–6]. However, they do not increase consistently with temperature in our experiments. Lu et al. found that these three ratios decrease with heating time at 200 °C while increase with heating time at 300 °C in their anhydrous pyrolysis experiments and interpreted this phenomenon as that the rate of generation of these compounds from kerogen is faster than the rate of isomerization reactions in the bitumen at 200 °C in hydrous pyrolysis [19]. Lewan et al. [10] and Peters et al. [11] observed the reversal phenomenon of isomerization ratio of terpanes and steranes with temperature in the hydrous pyrolysis experiments on source rocks and ascribed it to the differential isomerization level between the kerogen-bound and free compounds. Several earlier studies have documented that the isomerization rates of extractable hopanes and steranes are higher than those bound to kerogen [12–15]. According to these previous studies, the reasonable explanation on the common variation trend of these three ratios with temperature in our experiments could be as following: (1) at 240 °C, the hopanes and steranes which are weakly bound to kerogen, were easily released at the first few hours while those which are strongly bound to kerogen, were rarely released due to the low temperature during the remaining heating time; (2) at 280 °C, in addition to the weakly bound compounds which were released during the first few hours, the strongly bound ones were also released at a considerable rate during the later heating time; (3) at 320 °C, both the weakly and strongly bound compounds were released at the first few hours due to the high temperature. The critical point for this interpretation is that both hopanes and steranes are attached to kerogen via different types of bonds with different activation energy. Previous

Table 2
Molecular parameters for original extract and pyrolysates produced at various experimental conditions.

	1	2	3	4	5	6	7	8	9	10	11	12	13
Original	0.29	0.86	2.03	1.50	0.00	0.14	0.60	0.21	0.73	0.36	0.12	0.25	0.04
240 °C													
Ker-1	0.04	0.44	0.17	0.13	0.07	0.00	0.04	0.13	0.37	0.43	0.40	0.42	0.27
Ker-2	0.07	0.34	0.17	0.18	0.12	0.00	0.10	0.12	0.44	0.41	0.38	0.40	0.25
Kw-12	0.14	0.57	0.53	0.31	0.14	0.03	0.06	0.23	0.47	0.36	0.35	0.36	0.23
Kw-14	0.15	0.55	0.53	0.31	0.14	0.03	0.05	0.24	0.45	0.37	0.35	0.35	0.24
Kao-1	0.00	0.68	0.11	0.07	0.20	0.00	0.03	0.14	0.36	0.45	0.38	0.38	0.27
Kao-2	0.00	0.64	0.10	0.06	0.21	0.00	0.03	0.13	0.36	0.44	0.38	0.39	0.26
Mon-1	0.70	0.62	1.52	0.11	0.13	0.33	0.05	0.19	0.38	0.43	0.30	0.33	0.39
Mon-2	0.74	0.64	1.56	0.10	0.12	0.40	0.05	0.21	0.47	0.37	0.26	0.31	0.36
Cal-1	0.80	0.58	1.26	0.09	0.15	0.32	0.09	0.23	0.40	0.40	0.29	0.34	0.30
Cal-2	0.82	0.59	1.22	0.10	0.12	0.30	0.06	0.23	0.37	0.40	0.29	0.33	0.34
Dol-2	0.83	0.66	1.59	0.09	0.10	0.45	0.05	0.23	0.45	0.40	0.26	0.32	0.29
Dol-3	0.78	0.62	1.53	0.09	0.12	0.40	0.05	0.24	0.44	0.40	0.25	0.32	0.24
280 °C													
Ker-3*	0.00	0.17	0.00	0.00	0.00	0.00	0.00	0.00	0.51	0.46	0.36	0.40	0.15
Ker-5	0.00	0.12	0.00	0.00	0.00	0.00	0.00	0.00	0.48	0.45	0.35	0.43	0.13
Kw-15*	0.00	0.13	0.00	0.00	0.00	0.00	0.00	0.01	0.53	0.41	0.30	0.40	0.16
Kw-16	0.00	0.16	0.00	0.00	0.00	0.00	0.00	0.02	0.57	0.40	0.28	0.40	0.20
Kao-3*	0.00	0.26	0.00	0.00	0.00	0.00	0.00	0.02	0.55	0.38	0.29	0.33	0.15
Kao-4	0.00	0.25	0.00	0.00	0.00	0.00	0.00	0.02	0.55	0.36	0.28	0.32	0.15
Mon-3*	0.19	0.39	0.84	0.09	0.00	0.26	0.02	0.04	0.59	0.34	0.24	0.28	0.17
Mon-4	0.16	0.39	0.75	0.09	0.00	0.19	0.02	0.04	0.62	0.34	0.22	0.28	0.18
Cal-3*	0.24	0.37	1.00	0.17	0.00	0.35	0.04	0.04	0.61	0.30	0.21	0.26	0.24
Cal-4	0.22	0.38	0.98	0.15	0.00	0.20	0.03	0.04	0.59	0.31	0.23	0.28	0.22
Dol-4*	0.23	0.48	0.92	0.17	0.04	0.29	0.04	0.08	0.64	0.29	0.23	0.26	0.22
Dol-5	0.25	0.48	0.90	0.17	0.04	0.28	0.05	0.14	0.61	0.32	0.21	0.28	0.22
320 °C													
Ker-6*	0.00	0.11	0.00	0.00	0.00	0.00	0.00	0.00	0.29	0.51	nd	nd	0.00
Ker-7	0.00	0.11	0.00	0.00	0.00	0.00	0.00	0.00	0.33	0.57	nd	nd	0.00
Kw-17*	0.00	0.15	0.00	0.00	0.00	0.00	0.00	0.00	0.33	0.62	nd	nd	0.00
Kw-18	0.00	0.21	0.00	0.00	0.00	0.00	0.00	0.00	0.28	0.58	nd	nd	0.00
Kao-5*	0.00	0.09	0.00	0.00	0.00	0.00	0.00	0.00	0.42	0.56	0.41	0.42	0.13
Kao-7	0.00	0.07	0.00	0.00	0.00	0.00	0.00	0.00	0.42	0.57	0.41	0.44	0.14
Mon-7*	0.07	0.10	0.00	0.03	0.00	0.03	0.02	0.00	0.47	0.54	0.36	0.34	0.11
Cal-5*	0.06	0.11	0.00	0.03	0.00	0.02	0.05	0.01	0.51	0.54	0.36	0.33	0.13
Cal-6	0.04	0.09	0.00	0.01	0.00	0.02	0.01	0.01	0.49	0.53	0.34	0.32	0.14
Dol-6*	0.06	0.12	0.00	0.03	0.00	0.02	0.23	0.01	0.58	0.50	0.29	0.30	0.11
Dol-7	0.06	0.14	0.00	0.01	0.00	0.03	0.01	0.02	0.60	0.48	0.33	0.31	0.18

1: trisnorhopenes/trisnorhopanes=(22,29,30-trisnorneohop-13(18)-ene + 22,29,30-trisnorhop-17(21)-ene + unknown trisnorhopene)/ (18α(H),22,29,30- trisnorhopane + 17α(H),22,29,30-trisnorhopane + 17β(H),22,29,30-trisnorhopane); 2: 17β(H),22,29,30-trisnorhopane/17α(H),22,29,30-trisnorhopane; 3: (30-norneohop-13(18)-ene + 30-norhop-17(21)-ene)/17α(H),21β(H)-30-norhopane measured from *m/z* 396 and *m/z* 398 mass chromatograms; 4: 30-norneohop-13(18)-ene/(17α(H)21β(H)-30-norhopane + 30-norhop-17(21)-ene); 5: 17β(H)21β(H)-30-norhopane/(17α(H),21β(H)-30-norhopane + 30-norneohop-17(21)-ene); 6: hop-17(21)-ene/17α(H),21β(H)-hopane; 7: neohop-13(18)-ene/17α(H),21β(H)-hopane; 8: 17β(H)21β(H)-hopane/17α(H),21β(H)-hopane; 9: 17β(H)(21)α(H)-hopane/17α(H),21β(H)-hopane; 10: $C_{31}22S/(22R + 22S)$ homohopanes; 11: $C_{29}20S/(20R + 20S)$ steranes; 12: $C_{29}\alpha\beta\beta/(\alpha\alpha\alpha + \alpha\beta\beta)$ steranes; 13: ΣC_{29}steranes/17α(H),21β(H)-hopane; nd: not determined due to low abundances; Original: original extract from the initial shale; Ker-: kerogen alone; Kw-: kerogen plus de-ionized water (OC:water = 1:1.5 Wt.); Kao-: kerogen plus kaolinite and de-ionized water (OC:kaolinite:water = 1:24:7–10 Wt.); Mon-: kerogen plus montmorillonite and de-ionized water (OC:montmorillonite:water = 1:24:7–10 Wt.); Cal-: kerogen plus calcite and de-inonized water (OC:calcite:water = 1:24:7–10 Wt.); Dol-: kerogen plus dolomite and de-ionized water (OC:dolomite:water = 1:24:7–10 Wt.).
* For the samples within these capsules that Soxhlet extractions were performed subsequently after gas (C1–C5) hydrocarbon analyses, for the samples within the other capsules that Soxhlet extractions were performed subsequently after liquid (C8–C18) hydrocarbon analyses.

studies have revealed that terpenoids and steroids can be linked to kerogen by carbon–carbon bonds [30], ester and ether linkages [31–35], or sulphur bridges [33,36,37].

The few exceptions to the variation trend may be credited to the differential maturation rates for these compounds among the six experiments. Biomarker maturation could precede a step earlier in the experiments for kerogen alone and in the presence of de-ionized water only than the others. We can expect that the ratio of $C_{31}22S/(22R + 22S)$ homohopanes in the experiments for kerogen alone and in the presence of de-ionized water only may be higher at <240 °C than at 240 °C while lower at <280 °C than at 280 °C (Fig. 5a).

Previous studies have documented that the ratio of 17β(H),21α(H)-hopane/17α(H),21β(H)-hopane decreases with the thermal maturity or temperature [6]. In our experiments, this ratio increases from 240 °C to 280 °C, and then, decreases from 280 °C to 320 °C (Fig. 5d), inconsistent with the temperature. The explanation on this phenomenon could be the same as for the three ratios of $C_{31}22S/(22R + 22S)$ homohopanes and $C_{29}20S/(20R + 20S)$ and $C_{29}\alpha\beta\beta/(\alpha\alpha\alpha + \alpha\beta\beta)$ steranes. The ratio of ΣC_{29}steranes/17α(H),21β(H)-hopane decreases with temperature (Table 2), demonstrating that hopanes are more stable than steranes in our experiments in the temperature range from 240 °C to 320 °C.

4.3. Water effects

The abundances of hopenes and 17β(H)21β(H)-hopanes relative to the stable counterparts of 17α(H)21β(H)-hopanes and the ratios of $C_{31}22S/(22R + 22S)$ homohopanes, $C_{29}20S/(20R + 20S)$ steranes and $C_{29}\alpha\beta\beta/(\alpha\alpha\alpha + \alpha\beta\beta)$ steranes all demonstrate that the maturation rates of hopanoids and steranes are substantially higher in group 1 than in group 2 (Table 2, Figs. 1–5), which is consistent to the result of bitumen analysis [23]. Although the two experiments for kerogen alone and in the presence of de-ionized water only (OC:water 1:1.5) belong to the group 1, several significant differences can be observed in the distributions of hopanoids and steranes between these two experiments:

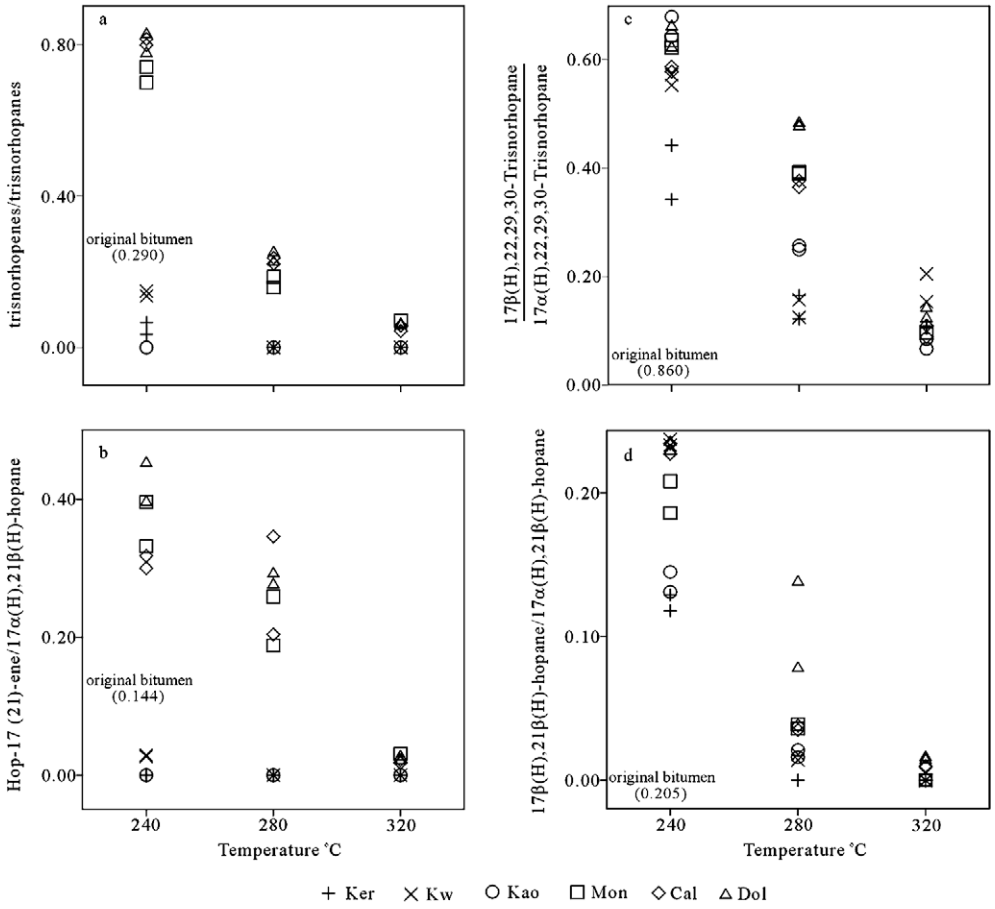

Fig. 4. Diagrams of the ratios of trisnorhopenes/trisnorhopanes, hop-17(21)-ene/17α(H),21β(H)-hopane, 17β(H),22,29,30-trisnorhopane/17α(H),22,29,30-trisnorhopane, and 17β(H)21β(H)-hopane/ 17α(H),21β(H)-hopane vs. temperature. Ker-, Kw-, Kao-, Mon-, Cal- and Dol- see Table 2.

(1) Trisnorhopenes/trisnorhopanes ratio is relatively lower in the experiment for kerogen alone than in the presence of de-ionized water only at 240 °C (Table 2, Figs. 1 and 4a).
(2) 17β(H),22,29,30-Trisnorhopane/17α(H),22,29,30-trisnorhopane ratio is much lower in the experiment for kerogen alone than in the presence of de-ionized water only at 240 °C (Table 2, Figs. 1 and 4c).
(3) 17β(H)21β(H)-Hopane/17α(H),21β(H)-hopane ratio is significantly lower in the experiment for kerogen alone than in the presence of de-ionized water only at 240 and 280 °C (Table 2, Figs. 1, 2 and 4d).
(4) (30-Norneohop-13(18)-ene + 30-norhop-17(21)-ene)/17α(H), 21β(H)-30- norhopane ratio is substantially lower in the experiment for kerogen alone than in the presence of de-ionized water only at 240 °C (Table 2, Fig. 1).
(5) All the three ratios of C_{31}22S/(22R + 22S) homohopanes, C_{29}20S/(20R + 20S) and C_{29}αββ/(ααα + αββ) steranes are relatively higher in the experiment for kerogen alone than in the presence of de-ionized water only at 240°C and 280°C (Table 2, Figs. 1, 2 and 5a–c).

These results demonstrate that the maturation rates of hopanoids and steranes are higher in the experiment for kerogen alone than in the presence of de-ionized water only. Therefore, water clearly retarded the maturation of these biomarker compounds during our experiments, consistent to the study by Lewan [21].

4.4. Mineral effects

Differences in the distributions of hopanoids and steranes are substantial between the experiment in the presence of kolinite (group 1) with low pH value (OC:kaolinite:water = 1:24:7–10, pH 4.99) and the group 2 in the presence of montmorillonite, calcite and dolomite with high pH value (OC:mineral:water 1:24:7–10, pH 8.84–9.88): the amounts of unstable hopenes and 17β(H)21β(H)-hopanes relative to stable 17α(H),21β(H)-hopanes are significantly lower while the ratios of C_{31}22S/(22R + 22S) homohopanes, C_{29}20S/(20R + 20S) steranes and C_{29}αββ/(ααα + αββ) steranes are significantly high in the former than latter (Table 2, Figs. 1–5). These results demonstrate that the maturation rates of these biomarker compounds are higher in the former than latter. As a similar amount of de-ionized water was added in all these four experiments (OC:mineral:water 1:24:7–10), the maturity differences can be only ascribed to the mineral acidity. The maturation rates of hopanoids and steranes were substantially accelerated under acidic condition while prohibited under alkaline condition in our experiments. This observation is consistent with many previous studies [11,16–20].

The maturation rates of hopanoids and steranes in the experiment in the presence of kaolinite (OC:kaolinite:water = 1:24:7–10) are similar to or slightly lower than that for kerogen alone while slightly higher than that in the presence of de-ionized water only (OC:water 1:1.5) based on the molecular parameters (Table 2, Figs. 4 and 5). We believe that the high amount of water could reduce the maturation rates, and therefore, counterbalance the acidic

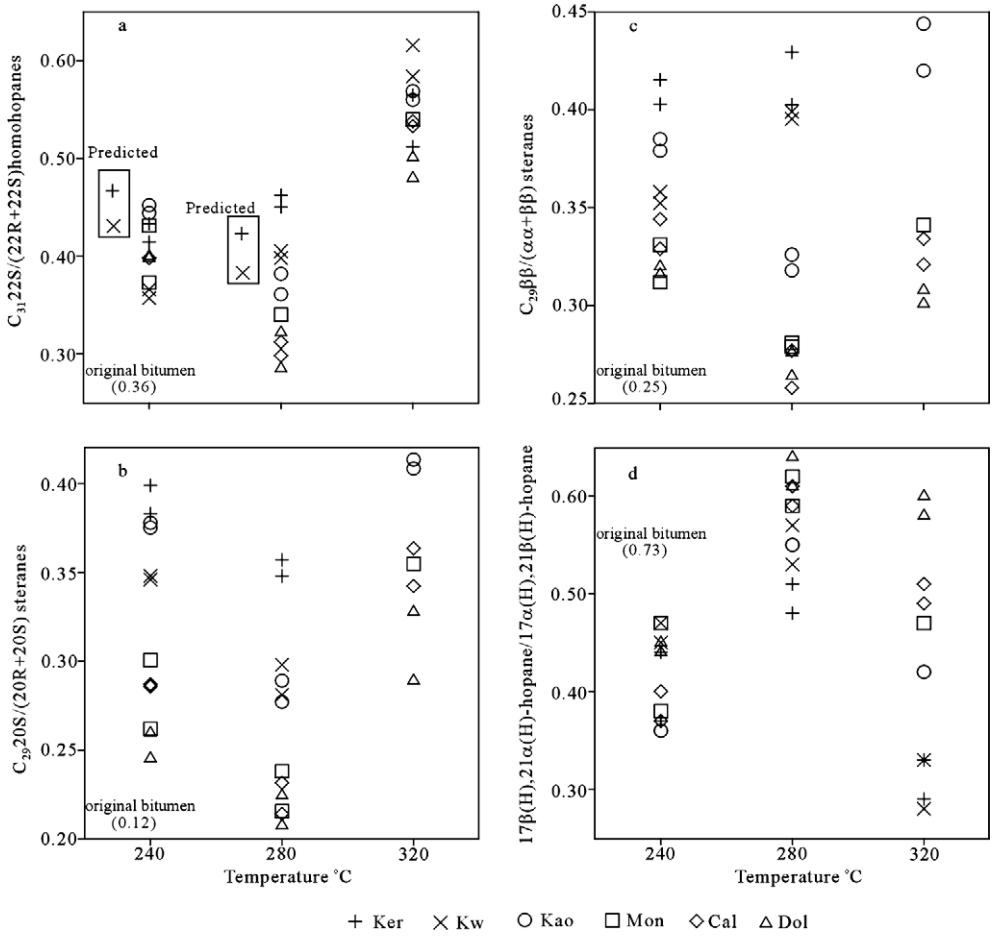

Fig. 5. Diagrams of the ratios of $C_{31}22S/(22R+22S)$ homohopanes, $C_{29}20S/(20R+20S)$ steranes, $C_{29}\alpha\beta\beta/(\alpha\alpha\alpha+\alpha\beta\beta)$ steranes, and 17β(H),21α(H)-hopane/17α(H),21β(H)-hopane vs. temperature. Ker-, Kw-, Kao-, Mon-, Cal- and Dol- see Table 2.

catalytic effect in the experiment in the presence of kaolinite, in comparison with the experiment for kerogen alone. In contrast, the maturation rates of hopanoids and steranes are substantially lower in the experiments in the presence of montmorillonite, calcite and dolomite than in the experiment for kerogen alone based on the molecular parameters (Table 2, Figs. 4 and 5). This result can be ascribed to the joint effects of water and mineral alkalinity (pH = 8.84–9.88). Both factors clearly retarded the maturation of hopanoids and steranes in our experiments.

5. Conclusions

(1) The maturation rates of hopanoids and steranes were accelerated with mineral acidity, but prohibited with the addition of water in our experiments.
(2) The concentrations of hopenes vary substantially among the six experiments at 240–28 °C. In contrast, 17β(H)21β(H)-hopanes are present in a relatively similar amount at 240 °C and have almost disappeared at 280 °C in all the six experiments. This result indicates that hopenes are more sensitive to the addition of excessive amount of water and pH value of minerals than are 17β(H)21β(H)-hopanes during our pyrolysis experiments.
(3) The reversal of the three ratios of $C_{31}22S/(22R+22S)$ homohopanes and $C_{29}20S/(20R+20S)$ and $C_{29}\alpha\beta\beta/(\alpha\alpha\alpha+\alpha\beta\beta)$ steranes at 280 °C implies that both hopanes and steranes are attached to kerogen via different types of bonds with different activation energy.

Acknowledgments

This project was funded by the state 973 Program of China (Grant No. G1999043307 and 2005CB422102) and the Earmarked Fund of the State Key Laboratory of Organic Geochemistry (Grant No. SKLOG2008A01). The authors are grateful to Drs Hongping He, Jianye Jia, Yangchuan Wang and Daqing Wu of Guangzhou Institute of Geochemistry for providing mineral samples with high purity as catalyst used in this study. This is contribution No. IS-1094 from GIGCAS.

References

[1] Peters KE, Walters CC, Moldowan JM. The biomarker guide, vol 2. In: Biomarkers and isotopes in petroleum exploration and earth history. UK: Cambridge University Press; 2005.
[2] Ensminger A, van Dorsselaer A, Spyckerelle D, Albrecht P, Ourisson G. Pentacyclic triterpenes of the hopane type as ubiquitous geochemical markers: origin and significance. In: Tissot B, Bienner F, editors. Advances in organic geochemistry 1973. Paris: Editions Technip; 1974. p. 245–60.
[3] Ensminger A, Albrecht P, Ourisson G, Tissot B. Evolution of polycyclic alkanes under the effect of burial (Early Toarcian shales, Paris basin). In: Campos R, Coni J, editors. Advances in organic geochemistry 1975. Madrid: Enadimsa; 1977. p. 45–52.
[4] Seifert WK. Steranes and terpanes in kerogen pyrolysis for correlation of oils and source rocks. Geochim Cosmochim Acta 1978;42:473–84.
[5] Seifert WK, Moldowan JM. Paleoreconstruction by biological markers. Geochim Cosmochim Acta 1981;45:783–94.
[6] Mackenzie AS, Patience RL, Maxwell JR, Vandenbroucke M, Durand B. Molecular parameters of maturation in the Toacian shales, Paris basin, France I. Changes in the configurations of the acyclic isoprenoid alkanes, steranes and triterpanes. Geochim Cosmochim Acta 1980;44:1709–21.

[7] Shi J, Mackenzie AS, Alexander R, Eglinton G, Gowar AP, Wolff GA, et al. A biological marker investigation of petroleum and shales from the Shengli Oilfield, The People's Republic of China. Chem Geol 1982;35:1–31.
[8] Ourisson G, Albrecht P, Rohmer M. The microbial origin of fossil fuels. Scientific American 1984;251:44–51.
[9] Qu D, Shi J, Xiang M. Novel extended side-chain-unsaturated hopenes released from the kerogen macromolecules under artificial conditions. Org Geochem 1996;24:815–23.
[10] Lewan MD, Bjorøy M, Dolcater DL. Effects of thermal maturation on steroid hydrocarbons as determined by hydrous pyrolysis of Phosphoria Retort Shale. Geochim Cosmochim Acta 1986;50:1977–87.
[11] Peters KE, Moldowan JM, Sundararaman P. Effects of hydrous pyrolysis on biomarker thermal maturity parameters: monterey phosphatic and siliceous members. Org Geochem 1990;15:249–65.
[12] Bishop AN, Abbott GD. The interrelationship of biological marker maturity parameters and molecular yields during contact metamorphism. Geochim Cosmochim Acta 1993;57:3661–8.
[13] Bishop AN, Love GD, Mcaulay AD, Snape CE, Farrimond P. Release of kerogen-bound hopanoids by hydropyrolysis. Org Geochem 1998;29:989–1001.
[14] Farrimond P, Bevan JC, Bishop AN. Hopanoid hydrocarbon maturation by an igneous intrusion. Org Geochem 1996;25:149–64.
[15] Love GD, Snape CE, Carr AD, Houghten RC. Release of covalently-bound alkane biomarkers in high yields from kerogen via catalytic hydropyrolysis. Org Geochem 1995;23:981–6.
[16] Sieskind O, Joly G, Albrecht P. Simulation of the geochemical transformations of sterols: superacid effect of clay minerals. Geochim Cosmochim Acta 1979;43:1675–9.
[17] Alexander R, Kagi RI, Larcher AV. Clay catalysis of alkyl hydrogen exchange reactions – reaction mechanisms. Org Geochem 1984;6:755–60.
[18] Tannenbaum E, Ruth E, Kaplan IR. Steranes and triterpanes generated from kerogen pyrolysis in the absence and presence of minerals. Geochim Cosmochim Acta 1986;50:805–12.
[19] Lu ST, Ruth E, Kaplan IR. Pyrolysis of kerogens in the absence and presence of montmorillonite – I. The generation, degradation and isomerization of steranes and triterpanes at 200 and 300 °C. Org Geochem 1989;14:491–9.
[20] Koopmans MP, Carson FC, Sinninghe Damsté JS, Lewan MD. Biomarker generation from Type II-S kerogens in claystone and limestone during hydrous and anhydrous pyrolysis. Org Geochem 1998;29:1395–402.
[21] Lewan MD. Experiments on the role of water in petroleum formation. Geochim Cosmochim Acta 1997;61:3691–723.
[22] Pan C, Geng A, Zhong N, Liu J, Yu L. Kerogen pyrolysis in the presence and absence of water and minerals. 1. Gas components. Energy Fuels 2008;22:416–27.
[23] Pan C, Geng A, Zhong N, Liu J, Yu L. Kerogen pyrolysis in the presence and absence of water and minerals: amount and compositions of bitumen and liquid hydrocarbons. Fuel 2009;88:909–19.
[24] Ensminger A. Evolution de composes poliycycliques sedimentaires. These de docteur en Sciences, Universite Louis Pasteur, Strasbourg, France; 1977.
[25] Brassell SC, Comet PA, Eglinton G, Isaacson PJ, McEvoy J, Maxwell JR, et al. The origin and fate of lipids in the Japan Trench. In: Douglas AG, Maxwell JR, editors. Advances in Organic Geochemistry 1979. Oxford: Pergamon Press; 1980. p. 375–92.
[26] Brault M, Simoneit BRT. Steroid and triterpenoid distributions in Bransfield Strait sediments: hydrothermally-enhanced diagenetic transformations. Org Geochem 1988;13:697–705.
[27] Baranger P, Disnar JR. Non-aromatic biomarkers associated with a palaeogene salt formation (Bresse, France). Org Geochem 1988;13:647–53.
[28] Larcher AV, Alexander R, Kagi RI. Differences in reactivities of sedimentary hopane diastereomers when heated in the presence of clays. Org Geochem 1988;13:665–9.
[29] Shi J, Wang B, Zhang L, Hong Z. Study on diagenesis of organic matter in immature rocks. Org Geochem 1988;13:869–74.
[30] Trifilieff S, Sieskind O, Albrecht P. Biological markers in petroleum asphaltenes: possible mode of incorporation. In: Moldowan JM, Albrecht P, Philp RP, editors. Biological markers in sediments and petroleum – a tribute to W. K. Seifert. Englewood Cliffs: Prentice Hall; 1992. p. 350–69.
[31] Mycke B, Narjes F, Michaelis W. Bacteriohopanetetrol from chemical degradation of an oil shale kerogen. Nature 1987;326:179–81.
[32] Michaelis W, Richnow HH, Jenisch C. Structural studies of marine and riverine humic matter by chemical degradation. Sci Total Environ 1989;81(/82):41–50.
[33] Farrimond P, Love GD, Bishop AN, Innes HE, Watson DF, Snape CE. Evidence for the rapid incorporation of hopanoids into kerogen. Geochim Cosmochim Acta 2003;67:1383–94.
[34] Jenisch A, Richnow HH, Michaelis W. Chemical structural units of macromolecule coal components. Org Geochem 1990;16:917–29.
[35] Richnow HH, Jenisch A, Michaelis W. Structural investigations of sulphur-rich macromolecular oil fractions and a kerogen by sequential chemical degradation. Org Geochem 1992;19:351–70.
[36] Sinnighe Damsté JS, Eglinton TI, Rijpstra WIC, de Leeuw JW. Characterization of organic sulphur compounds and sulphur-containing high molecular weight substances in sediments and immature crude oils. In: Orr WL, White CM, editors. Geochemistry of sulfur in fossil fuels, ACS symposium series, vol. 249; 1990. p. 486–528.
[37] Sinnighe Damsté JS, Rijpstra WIC, de Leeuw JW, Schenck PA. Origin of organic sulphur compounds and sulphur-containing high molecular weight substances in sediments and immature crude oils. Org Geochem 1988;13:593–606.